

Modeling the Control of Ribonucleotide Reductase

Joakim Widén



UPPSALA
UNIVERSITET

**Teknisk- naturvetenskaplig fakultet
UTH-enheten**

Besöksadress:
Ångströmlaboratoriet
Lägerhyddsvägen 1
Hus 4, Plan 0

Postadress:
Box 536
751 21 Uppsala

Telefon:
018 – 471 30 03

Telefax:
018 – 471 30 00

Hemsida:
<http://www.teknat.uu.se/student>

Abstract

Modeling the Control of Ribonucleotide Reductase

Joakim Widén

Ribonucleotide Reductase (RNR) is an enzyme that catalyzes the conversion of ribonucleotide diphosphates (NDPs) into deoxyribonucleotide triphosphates (dNTPs). The enzyme is essential for maintaining proper pool sizes of dNTPs which in turn is important for keeping mutation to a minimum.

The enzyme is allosterically regulated, which means that the products bind to it as effectors, altering the enzymes acceptibility of substrates, thus regulating their own production.

The enzyme system was simulated in Matlab with parameters determined in vitro and the behavior of the system was compared to previously published experiments. Although actual agreement between concentrations and parameters was difficult to establish, general agreement of the system's behavior with experimental results was noted.

Handledare: Emmeli Taberman
Ämnesgranskare: Måns Ehrenberg
Examinator: Elisabet Andrésdóttir
ISSN: 1650-8319, UPTEC STS05 006

SWEDISH ABSTRACT

SAMMANFATTNING PÅ SVENSKA

Ribonukleotidreduktas (eng. *ribonucleotide reductase*, förk. RNR) är ett enzym som reglerar tillförseln av deoxyribonukleotider (dNTP:er) till replikation och reparation av DNA i cellerna hos i stort sett alla organismer. Deoxyribonukleotiderna, som är byggstenar till DNA, finns i fyra olika former: dATP, dGTP, dCTP och dTTP. Det som skiljer dessa molekyler åt är vilka baser (adenin, guanin, cytosin och tymin) som de är uppbyggda kring.

Detta exjobb syftar till att kontrollera om den modell som föreslagits för regleringen av RNR fungerar vid simulering av enzymsystemet, dvs. om enzymet reglerar förekomsten av dNTP:er och dessutom är kapabelt till att hålla dNTP:erna på nivåer som observerats i levande celler.

En matematisk differentialekvationsmodell för regleringen av enzymet i en växande cell formulerades utifrån matematisk enzymkinetik och denna modell simulerades i Matlab. Resultaten från simuleringen jämfördes sedan med experimentella resultat från tidigare studier. Dessa jämförelser visade att RNR reglerar dNTP-koncentrationerna i cellen på ett rimligt sätt, även om jämförelser mellan exakta värden på parametrar och koncentrationer visade sig svåra att göra.

Modeling the Control of Ribonucleotide Reductase

Joakim Widén

May 27, 2005

Contents

1	INTRODUCTION	2
1.1	Aim of the Project	2
1.2	Methods and Data	2
1.3	Structure of the Report	3
2	RNR AND REDUCTION OF RIBONUCLEOTIDES	3
2.1	Reaction Overview	3
2.2	Allosteric Control	4
3	DESCRIPTION OF THE RNR MODEL	5
3.1	Michaelis-Menten Kinetics	5
3.2	Association of Effectors to the Enzyme	7
3.3	Implementation	10
3.4	External Control	10
3.5	Model of Replication	11
4	DETERMINATION OF PARAMETERS	11
4.1	Effector Dissociation Constants	12
4.2	Enzyme Reaction Constants	12
4.3	Verification of the Model Parameters	13
5	RESULTS AND COMPARISONS	16

1 INTRODUCTION

The DNA of all living organisms is constructed from four different deoxyribonucleotide phosphates (dNTPs), dATP, dGTP, dCTP and dTTP. In order to replicate and repair its DNA, the cell needs a steady supply of all of these dNTPs. Moreover, this supply has to be balanced for replication and repair to work properly. There are intrinsic metabolic pathways leading to the production of the dNTPs in the cell. Feedback and different types of regulation occur at different levels in these pathways, helping to maintain a balanced supply. This balance is very important for the cell to maintain, since perturbations in dNTP pools are associated with increased mutation frequencies and subsequent defects and diseases [1]. The focus of this thesis is on one such point of control.

1.1 Aim of the Project

The aim of this Master's thesis project has been to determine how a specific enzyme, *ribonucleotide reductase* (*RNR*), regulates the dNTP concentrations within this larger framework of pathways. There are many different classes of ribonucleotide reductases, depending on the organism of interest and on whether the reduction is aerobic or anaerobic. The focus of this study is the *Escherichia coli* aerobic enzyme, mainly because this is the most studied enzyme and therefore easiest to obtain data on.

1.2 Methods and Data

The model was simulated using differential equations describing the enzyme kinetics of RNR using Matlab, with a basic model structure already presented in a number of articles and reaction data from different *in vitro* experiments, all of which will be described later. The logic of the method has been to simulate the enzyme system using the known information and to compare the simulation results with the known *in vivo/in vitro* behavior of the system.

1.3 Structure of the Report

Chapter 2 will introduce reduction of ribonucleotides and the role of RNR in that process. Chapter 3 describes the model of the RNR enzyme action. Chapter 4 describes how the model parameters were obtained and applied to the model structure. Chapter 5, finally, presents the results of some runs with the simulated system and comparisons with the known behavior of the enzyme system.

2 RNR AND REDUCTION OF RIBONUCLEOTIDES

2.1 Reaction Overview

Reichard [1] presents an overview of the pathway of synthesis of dNTPs, which is the general path of synthesis in all organisms. This is shown in figure 1. Small molecules form ribonucleotides which are reduced to deoxyribonucleotides by the ribonucleotide reductase enzyme. The dNDPs (deoxyribonucleotide diphosphates) are formed directly by the RNR and in a subsequent phosphorylation reaction dNTPs are formed, which are then ready for use in DNA replication or repair.

**Small molecules → Ribonucleotides
→ Deoxyribonucleotides → DNA**

Figure 1: Overview of DNA synthesis. From [1].

A more detailed scheme, showing more reactions, is depicted in figure 2. This is also a simplification compared to the total scheme of reactions. As described in [1], the number of enzymes involved in the reduction of NDPs is much larger. In mammals, the number of relevant enzymes, according to Reichard, is seven. However, it can be argued that only the RNR enzyme and the dCTP aminase (see figure 2) are interesting when we are modeling the regulation of the dNTP concentrations, since these two enzymes are the only ones that are subject to control.

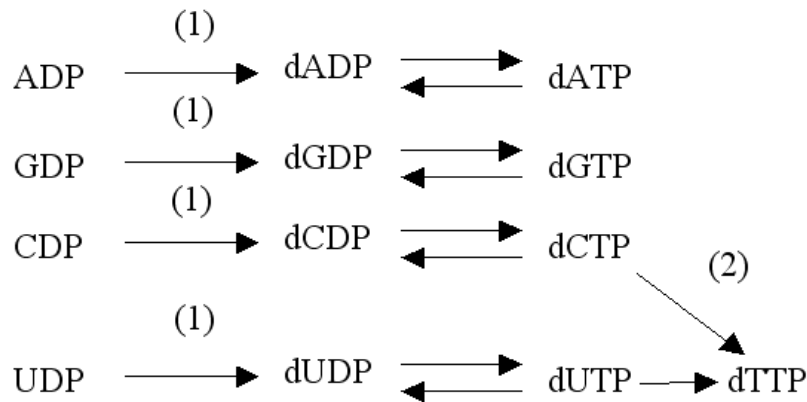


Figure 2: Pathway of deoxyribonucleotide synthesis. Reactions marked with (1) are catalyzed by ribonucleotide reductase and the reaction marked with (2) is catalyzed by dCTP deaminase. The total enzyme activity is considered to be controlled by the allosteric mechanism of RNR.

2.2 Allosteric Control

The control of the RNR and the deaminase is *allosteric*, meaning that the products of the enzymes bind back to them and alter the three-dimensional conformation of the protein so that the substrate specificity is changed. This means that when a product has been formed, it can bind back and change the enzyme structure, so as to negatively control its own production.

RNR of *E. coli* is controlled allosterically according to table 1. It has two so-called allosteric sites to which the effectors (dNTPs and ATP in this case) bind. The *activity site* regulates the overall activity of the enzyme, with ATP stimulating and dATP inhibiting the catalytic activity. The *specificity site* controls which NDPs are reduced by the enzyme. With ATP, dATP, dTTP or dGTP bound to this site, different substrates are accepted by the enzyme, as can be seen in table 1. Note that three out of four of the products of the enzyme bind to it as effectors, thereby regulating their own production from NDPs.

This model for the allosteric regulation has been verified experimentally in [2], [3] and [4], and described in a number of articles too large to present here. A recent review discussing the regulation of the enzyme can be found in [5].

Activity site	Specificity site	Reduction of
ATP	ATP, dATP	CDP, UDP
ATP	dTTP	GDP
ATP	dGTP	ADP
dATP	Any effector	Inhibition

Table 1: Allosteric regulation of ribonucleotide reductase. From [5].

dCTP aminase is also allosterically controlled, but in a much simpler way. dCTP (the product) binds in as positive effector, activating the enzyme and dTTP binds to it as negative effector, inhibiting the enzyme function [1].

3 DESCRIPTION OF THE RNR MODEL

In this section, a description of the model for the RNR enzyme function that is presented. It should be noted that this modeling and the subsequent evaluation, bug-fixing, *etc.* took up most of the thesis work. Therefore it takes up relatively much space in the report as well.

3.1 Michaelis-Menten Kinetics

Based on the general Michaelis-Menten formula for enzyme kinetics (see for example [8]), expressions can be derived for the production rates of dNTPs over the enzyme. Assuming Michaelis-Menten kinetics for the enzyme, the following are the inflows into the dNTP pools for the ADP- and GDP-reducing enzyme forms.

$$j_{dATP} = \frac{[RNR_{ADP}][ADP]k_{cat,ADP}}{[ADP] + K_{m,ADP}} \quad (1)$$

$$j_{dGTP} = \frac{[RNR_{GDP}][GDP]k_{cat,GDP}}{[GDP] + K_{m,GDP}} \quad (2)$$

$[dNTP]$, $[NDP]$ and $[RNR_{NDP}]$ for $N = A, G$ denote effector, substrate and enzyme concentrations, respectively. The k_{cat} constants are the maximum

velocities of the enzyme reactions and the K_m constants are the substrate concentrations at which the enzyme reaction reaches half of its maximum velocity. The case for the CDP- and UDP-reducing forms of the enzyme is a bit more complicated, since the same form of enzyme reduces either of these substrates, so that the substrates compete for the binding sites on the enzyme. Denoting the flow over each type of substrate reduction reaction j and i , the k_{cat} and K_m values for the two reactions $k_{cat,i}$, $k_{cat,j}$, $K_{m,i}$ and $K_{m,j}$, the substrates and enzyme concentrations s_1 , s_2 and e , respectively, and the enzyme-substrate complexes es_1 and es_2 , the following relations hold:

$$e = \frac{j}{k_{cat,j}} \frac{K_{m,j}}{s_1}, es_1 = \frac{j}{k_{cat,j}} \quad (3)$$

$$e = \frac{i}{k_{cat,i}} \frac{K_{m,i}}{s_2}, es_2 = \frac{i}{k_{cat,i}} \quad (4)$$

$$e_0 = e + es_1 + es_2 \quad (5)$$

From these relations, the following formulas for the flows can be derived:

$$j = \frac{e_0 s_1 k_{cat,j}}{K_{m,j} + s_1 + \frac{K_{m,j} s_2}{K_{m,i}}}, i = \frac{e_0 s_2 k_{cat,i}}{K_{m,i} + s_2 + \frac{K_{m,i} s_1}{K_{m,j}}} \quad (6)$$

In terms of RNR and NDP concentrations, the reduction rates of CDP and UDP become:

$$j_{dCTP} = \frac{[RNR_{CDP,UDP}][CDP]k_{cat,CDP}}{[CDP] + K_{m,CDP} \left(1 + \frac{[UDP]}{K_{m,UDP}}\right)} \quad (7)$$

$$j_{dTTP} = \frac{[RNR_{CDP,UDP}][UDP]k_{cat,UDP}}{[UDP] + K_{m,UDP} \left(1 + \frac{[CDP]}{K_{m,CDP}}\right)} \quad (8)$$

As can be seen, apart from the regulation of RNR, it is the ratios k_{cat}/K_m and $[CDP]/[UDP]$ that determines which substrate is reduced. In the context

of a growing cell, there will also be a dilution effect due to growth, which is taken into account by subtraction of a dilution term $\mu[dNTP]$ from each equation above, where μ is the exponential growth rate (see for example [9]).

3.2 Association of Effectors to the Enzyme

When modeling the action of the allosterically regulated RNR over time, two separate events must be taken into consideration: (1) the reduction of NDPs by the enzyme, modeled by the Michaelis-Menten kinetics above, and (2) the association and dissociation of dNTPs to and from the enzyme. These two events are obviously intertwined, since production of new dNTPs will affect the amount of free dNTPs that can bind to the enzyme, and since altered ratios of forms of RNR, resulting from dNTP concentration changes, will change the production rates of the different dNTPs.

It seems reasonable to use the method of *separation of timescales* (see [8]), in which we assume that the two events occur on different time scales, so that equilibrium concentrations of effector-enzyme complexes, free dNTPs and free enzymes stabilize instantly in relation to the production flows over the enzyme. That is, as soon as new dNTPs are produced by the enzyme, they immediately reach equilibrium with the enzyme.

Thus, the problem of calculating effector concentrations at a given time point reduces to solving a system of equilibrium concentrations. With $K_{d,X,Y}$ being the dissociation constant for effector site X and effector Y , and $[SPEC_Y]$ and $[ACT_Y]$ denoting the concentrations of the specificity site and activity site for an effector Y (subscript *free* indicating that no effector is bound) the following six equations describe binding of effectors to the RNR. (The dissociation constants describe the dissociation of enzyme-effector complexes. The greater the value of the dissociation constant, the larger the ratio of free effector and enzyme. See [8] for further discussion.)

$$\frac{[ACT_{free}][dATP]}{[ACT_{dATP}]} = K_{d,ACT,dATP} \quad (9)$$

$$\frac{[ACT_{free}][ATP]}{[ACT_{ATP}]} = K_{d,ACT,ATP} \quad (10)$$

$$\frac{[SPEC_{free}][dATP]}{[SPEC_{dATP}]} = K_{d,SPEC,dATP} \quad (11)$$

$$\frac{[SPEC_{free}][ATP]}{[SPEC_{ATP}]} = K_{d,SPEC,ATP} \quad (12)$$

$$\frac{[SPEC_{free}][dGTP]}{[SPEC_{dGTP}]} = K_{d,SPEC,dGTP} \quad (13)$$

$$\frac{[SPEC_{free}][dTTP]}{[SPEC_{dTTP}]} = K_{d,SPEC,dTTP} \quad (14)$$

In addition to these, the *law of mass conservation* (which states that the total amounts of enzyme and effectors, *i.e.* in both bound and unbound states, are preserved and thus constant) gives us the following relations:

$$[dATP] + [ACT_{dATP}] + [SPEC_{dATP}] = [dATP]_{tot} \quad (15)$$

$$[ATP] + [ACT_{ATP}] + [SPEC_{ATP}] = [ATP]_{tot} \quad (16)$$

$$[dGTP] + [SPEC_{dGTP}] = [dGTP]_{tot} \quad (17)$$

$$[dTTP] + [SPEC_{dTTP}] = [dTTP]_{tot} \quad (18)$$

$$[ACT_{dATP}] + [ACT_{ATP}] = [RNR]_{tot} \quad (19)$$

$$[SPEC_{dATP}] + [SPEC_{ATP}] + [SPEC_{dGTP}] + [SPEC_{dTTP}] = [RNR]_{tot} \quad (20)$$

To calculate the concentrations of the different forms of RNR, we use these equilibrium concentrations, together with the information given in table 1. Thus, the probability that RNR is in the form that reduces ADP is equal to the probability that ATP is bound to the activity site at the same time as dGTP is bound to the specificity site, i.e.

$$P(\text{ADP reduction}) = P(\text{ATP at ACT site})P(\text{dGTP at SPEC site}) \quad (21)$$

Similarly,

$$P(\text{GDP reduction}) = P(\text{ATP at ACT site})P(\text{dTTP at SPEC site}) \quad (22)$$

and

$$P(\text{CDP and UDP reduction}) = P(\text{ATP at ACT site})[P(\text{ATP at SPEC site}) + P(\text{dATP at SPEC site})] \quad (23)$$

and, since the probabilities add up to 1,

$$P(\text{RNR inhibited}) = 1 - P(\text{ADP reduction}) - P(\text{GDP reduction}) - P(\text{CDP and UDP reduction}) \quad (24)$$

We can express the above probabilities for effector binding as concentration ratios on the form, for example

$$P(\text{ATP at ACT site}) = \frac{[ACT_{ATP}]}{[RNR]_{tot}} \quad (25)$$

and so on. Substituting into the probability equations for RNR reduction and multiplying each equation with $[RNR]_{tot}$ (see Appendix 2: Computational Methods) gives us the following expressions for the RNR concentrations (as above, RNR_Y denotes the enzyme form reducing substrate Y):

$$[RNR_{GDP}] = \frac{[ACT_{ATP}][SPEC_{dTTP}]}{[RNR]_{tot}} \quad (26)$$

$$[RNR_{ADP}] = \frac{[ACT_{ATP}][SPEC_{dGTP}]}{[RNR]_{tot}} \quad (27)$$

$$[RNR_{CDP,UDP}] = \frac{[ACT_{ATP}]([SPEC_{ATP}] + [SPEC_{dATP}])}{[RNR]_{tot}} \quad (28)$$

$$[RNR_{inhibited}] = [RNR]_{tot} - [RNR_{GDP}] - [RNR_{ADP}] - [RNR_{CDP,UDP}] \quad (29)$$

3.3 Implementation

The actual simulation proceeds according to the following steps (this is only a basic structure; between steps 1 and 2 there also comes in for example consumption of dNTP pools by DNA replication, depending on the purpose of the simulation):

at each time step

1. Calculate dNTP concentrations from Michaelis-Menten equations (1)-(2), (7)-(8).
2. Solve the equation system (9)-(20) to obtain effector (dNTP) and effector-site concentrations.
3. Calculate new RNR concentrations according to equations (26)-(29).

The M.M.-reactions are simulated using a simple Euler method, and for calculating the equilibrium concentrations in the partially non-linear equation system (9)-(20), Newton's method for multidimensional systems is employed. The exact code is attached in Appendix 1.

3.4 External Control

The conversion of dCTPs to dTTPs was modeled similarly by flowbased enzyme kinetics. The scheme in figure 3 describes the reactions over the deaminase enzyme. From this scheme the following expression for the flow can be derived (see Appendix 2: Computational Methods):

$$j = ECk_T = \frac{E_0k_TC/K_C}{1 + C/K_C + T/K_T} \quad (30)$$

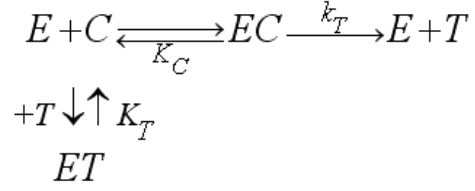


Figure 3: dCTP demainase reaction scheme. $C = [dCTP]$ and $T = [dTTP]$ and E is the free concentration of the enzyme. K_C and K_T are equilibrium constants for binding of dCTP and and dTTP to the enzyme and k_T is the rate constant for dCTP conversion by the enzyme.

3.5 Model of Replication

The outflow to replication was modeled as follows. With $K_{m,pol,dATP}$ being the K_m values for the polymerase reaction with dATP, and f_{dATP} the fraction of dATPs among the total amount of dNTPs being incorporated into the DNA, and so on for the other dNTPs, the following expression describes the flow to replication [10]:

$$j_{repl,dnTP} = \frac{f_{dnTP} D}{\frac{1}{k_{repl}} \sum_{i=A,C,G,U} (f_{diTP} (1 + \frac{K_{m,pol,diTP}}{[diTP]}))}, \quad (31)$$

$$n = A, C, G, U$$

This formula is derived in appendix 2. Here, k_{repl} is the maximum rate constant for replication, set to 1000 s^{-1} , and D is the number of replication forks, set to $0.1 \mu M$.

4 DETERMINATION OF PARAMETERS

Thus far we have only dealt with theoretical modeling of the enzyme reactions and binding equilibriums. This section briefly describes how the reaction and binding constants were chosen, based on the available literature and scientific articles.

4.1 Effector Dissociation Constants

Ormö and Sjöberg calculated dissociation constants for the various effectors already presented in table 1 [6]. They used measured binding at 25 degrees C. Their values for the binding constants were used, since it was (as far as was possible to determine) the most recent article on the subject. One thing should be noted; in table 1 it is evident that both ATP and dATP can bind to both allosteric sites. However, Ormö and Sjöberg only measured separate binding for dATP but not for ATP. The binding of ATP to the enzyme as a whole was $80 \mu M$, according to their measurements, and this was used as binding constant to both sites.

The values of the constants are shown in table 2.

Constant	Value (μM)
$K_{d,ACT,dATP}$	6
$K_{d,SPEC,dATP}$	0.86
$K_{d,ACT,ATP}$	80
$K_{d,SPEC,ATP}$	80
$K_{d,dTTP}$	1.9
$K_{d,dGTP}$	0.77

Table 2: Effector dissociation constants from [6].

4.2 Enzyme Reaction Constants

Larsson and Reichard ([2], [3], [4]) measured K_m values for RNR with different effectors bound to it. From some of their other measurements it is also possible to calculate the corresponding k_{cat} values. It should be noted here also, that the information on experiment conditions given in these articles is far from clear-cut, so a significant amount of deciphering had to be done before the given data could even be used.

It will only be briefly described how the k_{cat} values that were used in the model were calculated. V_{max} (the maximum enzyme reaction rate) is given for each enzyme reaction. Since $e_0 k_{cat} = V_{max}$ (see [8]) we can calculate k_{cat} if we know the total amount of enzyme (e_0) in each experiment. The problem here is that the RNR enzyme consists of two subgroups which were given in unequal amounts in the different experiments, in some cases the difference

being as much as two times. The assumption has been that the subgroup with the lowest concentration was limiting, so that we can set it equal to the e_0 concentration. How accurate this assumption is can only be determined if we study the association of the subgroups to each other at different mutual concentrations. This, however, was rightly considered to be outside the scope of this thesis.

The K_m and k_{cat} values that finally came to be used are given in table 3.

Constant	Value
$K_{m,CDP}$	180 μM
$K_{m,UDP}$	220 μM
$K_{m,GDP}$	25 μM
$K_{m,ADP}$	30 μM
$k_{cat,CDP}$	0.3 s^{-1}
$k_{cat,UDP}$	0.25 s^{-1}
$k_{cat,GDP}$	0.17 s^{-1}
$k_{cat,ADP}$	0.17 s^{-1}

Table 3: K_m and k_{cat} values from [2], [3] and [4].

4.3 Verification of the Model Parameters

Now that we have a model describing the RNR enzyme system, calibrated with parameters from actual in vitro experiments, we should be able to easily verify this model construction by comparing it with the actual experiments of the aforementioned articles. This is possible, but not to a large extent, because sadly enough the experiments are so poorly presented in the articles that a direct comparison of results in most cases is virtually impossible. Also, in some cases the model does not manage to handle the extreme concentrations of the experiments. Possibly, this is because the experiments were performed in vitro while the model is supposed to describe the in vivo behavior. Also the fact that we are using a relatively simple Euler method could also cause this.

The experiments shown in figures 4 to 7 are instructive. The agreement is not perfect, but at least the behavior of the model resembles the experimental behavior of the in vitro system, which is a good sign. For example, the dATP and dCTP curves are similar. Note that in figure 4 the linearity of the

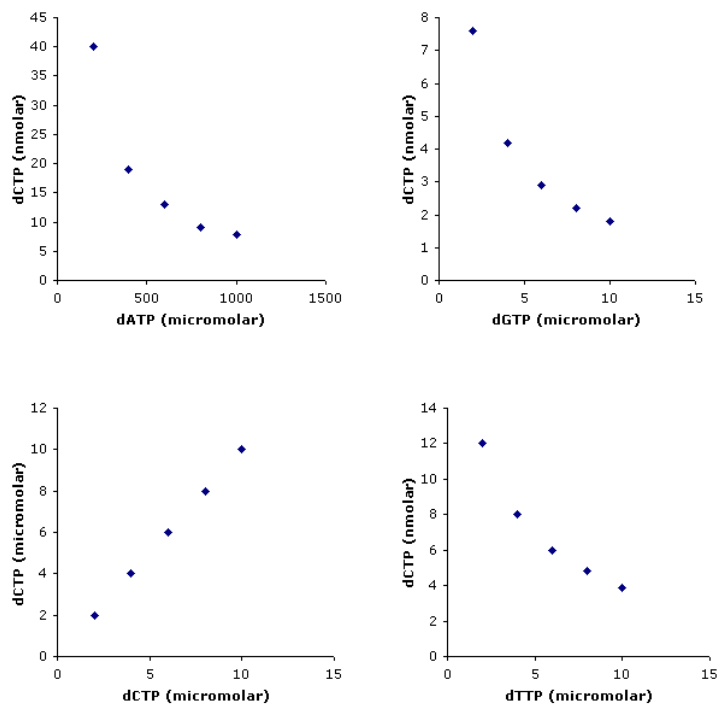


Figure 4: Effects of different dNTPs on CDP reduction. Simulations were performed with the following parameter values (μM): ATP 1.5, CDP 500, RNR 0.53. dNTP concentrations were increased successively and the dCTP produced by the enzyme system was stored and plotted. This is to be compared to the next figure.

dCTP curve almost exclusively is due to the added dCTP, and the curve of produced dCTP is virtually constant, as in figure 5. The dTTP and dGTP curves are not similar, however, increasing and constant as they are in figure 5, while decreasing in figure 4.

Given the model structure, the result in figure 4 is obviously the expected one, with dATP initially stimulating the reduction heavily and in greater concentrations inhibiting it by binding to the activity site of the RNR, and the other dNTPs inhibiting the enzyme action. Figure 5, which shows the experimental result used to deduce the model thus seems to contradict it (apart from the agreement between the dATP curves) most clearly with dTTP stimulating CDP reduction, whereas it should in fact inhibit it according to the model (see table 1).

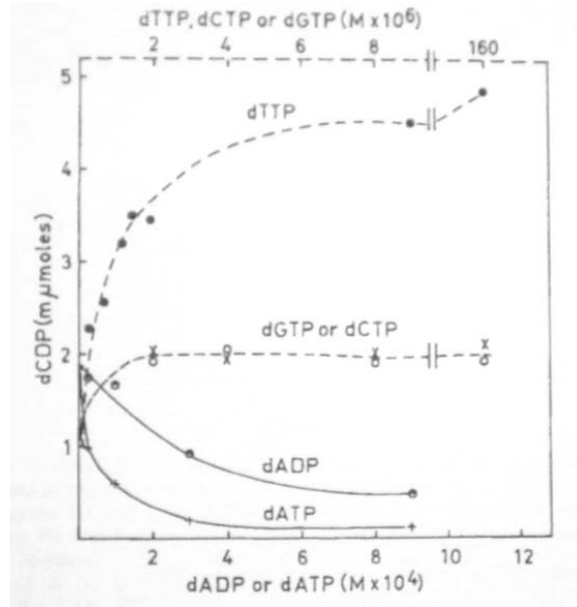


Figure 5: Effects of different dNTPs on CDP reduction. From [2]. dNTPs were successively added to a solution containing enzyme, NDPs and ATPs in quantities as in the previous figure. The dCDP produced by the enzyme was measured. This is to be compared to the previous figure.

The agreement is better in figures 6 and 7, although the actual values are difficult to compare. The important thing to note here is that the slope of the curves increases approximately equally with decreasing CDP concentrations in both figures.

The steady-state concentrations of the dNTPs were studied when simulating the system with the parameters given above. These concentrations are shown in figure 8. Other parameters, if not described above, can be found in table 5. When not otherwise stated, those values are used in this and subsequent figures. Conversion of dCTP to dTTP via the dCTP deaminase was not used here.

Figure 8 shows that the concentrations are differing quite heavily from each other, with differences amounting to several orders of magnitude. This behavior, with dATP, dGTP, dTTP and dCTP in increasing order, is preserved, more or less, when the above parameters are changed, even when the changes are huge. This suggests that the system is quite robust against changes in the model reaction and equilibrium parameters, but also that we do not seem to be able to "tune" the dNTP pools, so as to make them assume any value.

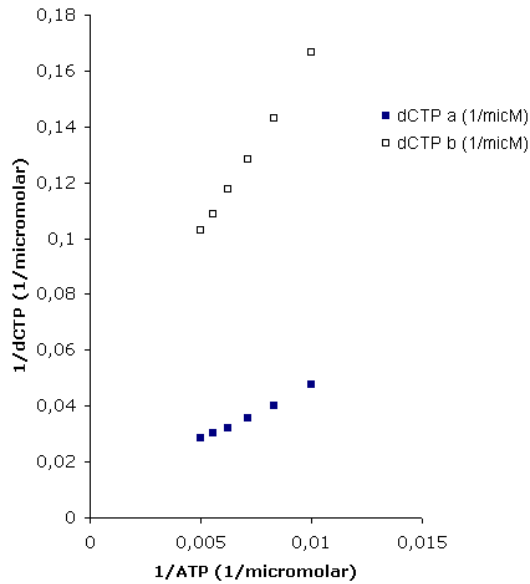


Figure 6: Effects of ATP on CDP reduction. Simulations were performed with the following parameter values (μM): RNR 0.53 and CDP 50 (curve a) and 500 (curve b). This is to be compared to the next figure.

This will be further discussed below.

5 RESULTS AND COMPARISONS

This chapter summarizes the conclusions that can be drawn about how the model works when tested against what is expected. In the example runs with the model (figures 8 to 12) the inflow of substrates (NDPs) were held constant and the outflow was modeled as in section 3.5. The figures show that dNTP concentrations all reach steady state values due to regulation (figure 8) and that effectors bind in to the allosteric sites in differing concentrations and reach steady state to maintain the control of the pools (figures 9 and 10). Figure 11 shows the concentrations of the RNR forms with different substrate specificity resulting from the binding of effectors to the allosteric sites. Note that the enzyme is active although the dATP concentration is relatively high (cfr. figure 8). This is because the intracellular concentration of ATP is set to the high in vivo value (3 mM, see [11]). Figure 12, finally, shows the resulting outflow of dNTPs to replication maintained by the RNR.

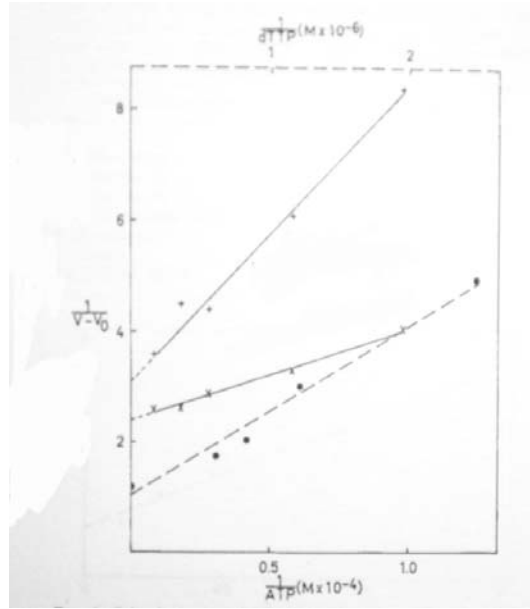


Figure 7: Effects of ATP on CDP reduction. From [2], with the same experimental conditions as in figure 5. The curve marked with + was measured with a CDP concentration of $50 \mu M$ and the one marked with \times with a CDP concentration of $500 \mu M$. This is to be compared to the previous figure.

One result that seems to be well in agreement with the experimental results is that dCTP is the largest pool as compared to the others, when the external deaminase control is not taken into account. When dilution is not modeled (so that not all concentrations reach steady state values), the dCTP concentration increases infinitely.

As Reichard concludes in [1], only dCTP does not bind to any allosteric site, and thus it cannot regulate its own production. Instead, he writes, dCTP acts allosterically on the deaminase and it has been shown in experiments that cells lacking this pathway have an increased dCTP pool and a decreased dTTP pool. As shown with the model this is precisely what happens when simulating the system. This is most clearly so in the simulation without growth. However, without the external control through the deaminase pathway, the dTTP pool is not depleted, and as already has been concluded it is apparent that altering the ratio between dTTP and dCTP does not introduce any notable change in the other dNTP pools.

As a guideline, simulation outputs were compared with a set of dNTP pool concentrations that seem rather reasonable. They are taken from [7] and

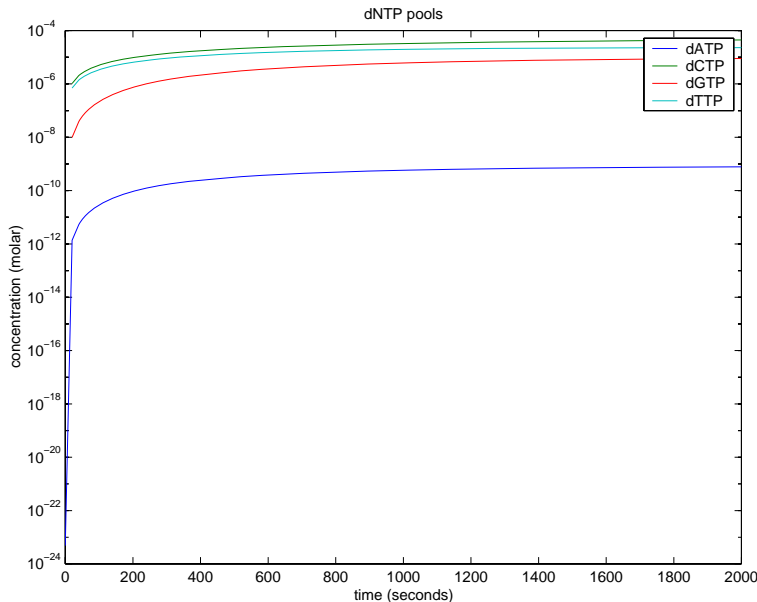


Figure 8: Steady state concentrations of dNTPs. Simulation with parameters shown in table 5.

are shown in table 4. We can see that with the parameter value choices of the simulation described above, the dNTP pools end up at much lower concentrations than the ones in table 4 (cfr. figure 8). They differ at least at three orders of magnitude, which is too much. Heavily increasing the amount of RNR (standard is $1 \mu M$) changes this to some degree, but it is not enough, and such an increase in the enzyme concentration is simply not reasonable.

dNTP pool	Concentration (μM)
dATP	180
dCTP	120
dGTP	70
dTTP	80

Table 4: dNTP pools from [7].

But perhaps we should not be surprised. Experimentally measured concentrations of the dNTP pools differ heavily according to Reichard: "It is not possible to define a 'proper' size for a given dNTP pool. Reports from different laboratories vary considerably, apparently also for one and the same cell line." [1] And right there is one important problem of verifying the model: neither the parameters nor the data against which to verify the model are

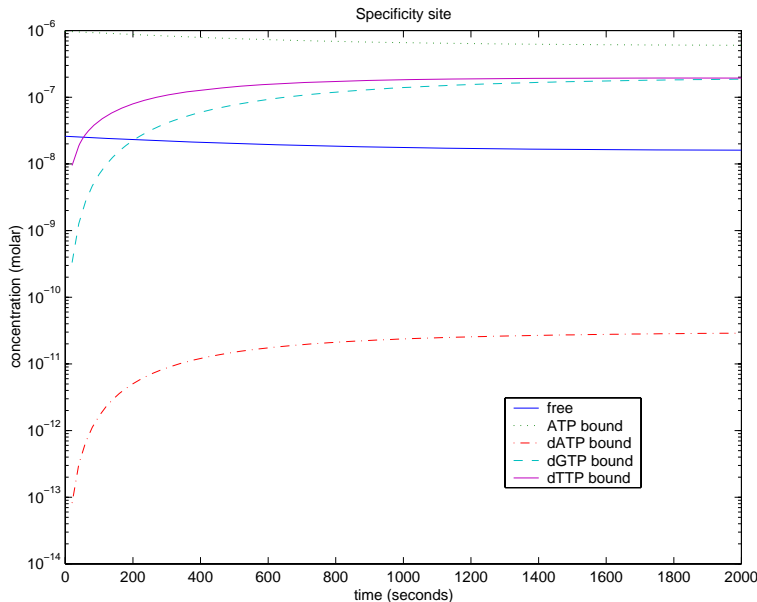


Figure 9: Effectors bound to the specificity site of the RNR enzyme. Total RNR concentration is 1 M. Simulation with parameters shown in table 5.

confident. This is also because in vitro parameters are used for modeling in vivo behavior. Thus, we cannot really say if the parameter values (or the structure of the allosteric control) is correct, since we have no confident data to compare it with, and therefore we cannot answer the more important question of whether the RNR system is sufficient to explain the dNTP pool regulation. New in vivo experiments would certainly improve the chances of verifying the model.

Nevertheless, it is interesting to look at the robustness of the model. How does it respond to changes in inflow and outflow?

Figure 13 shows the results. The inflow of NDPs was heavily decreased for each NDP successively (by four orders of magnitude). As a result, the outflows were reduced by at least 6 orders of magnitude as compared to the previous figures. This indicates that the system is not robust towards changes in substrate pools. Changes in outflow to replication were also tested, but the model was not able to handle these.

To summarize, this has given insight to how the RNR enzyme works. Agreement with experimental results has been seen, especially for the dCTP pool size, but it has been difficult to draw any confident conclusions on the ex-

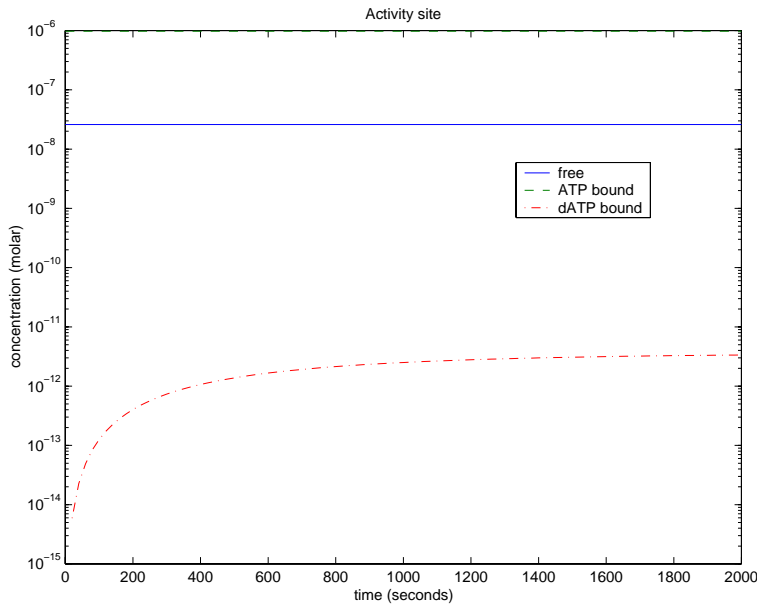


Figure 10: Effectors bound to the activity site of the RNR enzyme. Total RNR concentration is 1 M. Simulation with parameters shown in table 5.

act agreement between the model and experiments, since the experimental material available for comparison leaves many questions unanswered and unanswerable.

References

- [1] Reichard, P., "Interactions Between Deoxyribonucleotide and DNA Synthesis", *Ann. Rev. Biochem.* 1988 57:349-74.
- [2] Reichard, P., Larsson, A., "Enzymatic Studies of Deoxyribonucleotides IX", *J. Biol. Chem.* 1966 241:2533-2539.
- [3] Reichard, P., Larsson, A., "Enzymatic Studies of Deoxyribonucleotides X", *J. Biol. Chem.* 1966 241:2540-2549.
- [4] Reichard, P., Brown, N. C., "Role of Effector Binding in Allosteric Control of Ribonucleoside Diphosphate Reductase", *J. Mol. Biol.* 1969 46:39-55.

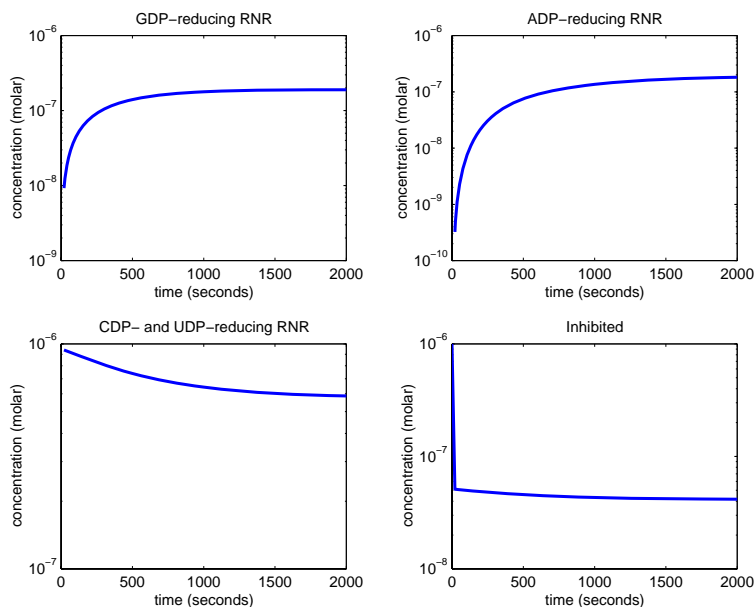


Figure 11: RNR with different substrate specificities. Simulation with parameters shown in table 5.

[5] Reichard, P., "Ribonucleotide Reductases: The Evolution of Allosteric Regulation", *Arch. Biochem. Biophys.* 2002 397:149-55.

[6] Ormö, M., Sjöberg, B., "An Ultrafiltration Assay for Nucleotide Binding to Ribonucleotide Reductase", *Analytical Biochem.* 1990 189:138-141.

[7] Kornberg, A., Baker, Tanja A., *DNA Replication, 2nd Edition*. San Francisco 1980.

[8] Berg, O., Ehrenberg, M., Lovmar, M., *Biophysical Chemistry*. Department of Cell and Molecular Biology. Uppsala University 2002.

[9] Ehrenberg, M., Elf, J., *Modeling of Molecular Control Systems*. Department of Cell and Molecular Biology. Uppsala University 2003.

[10] Emmeli Taberman, personal communication.

[11] Neidhardt, F. C., *Escherichia coli and Salmonella : cellular and molecular biology. Vol. 2*. Washington 1996.

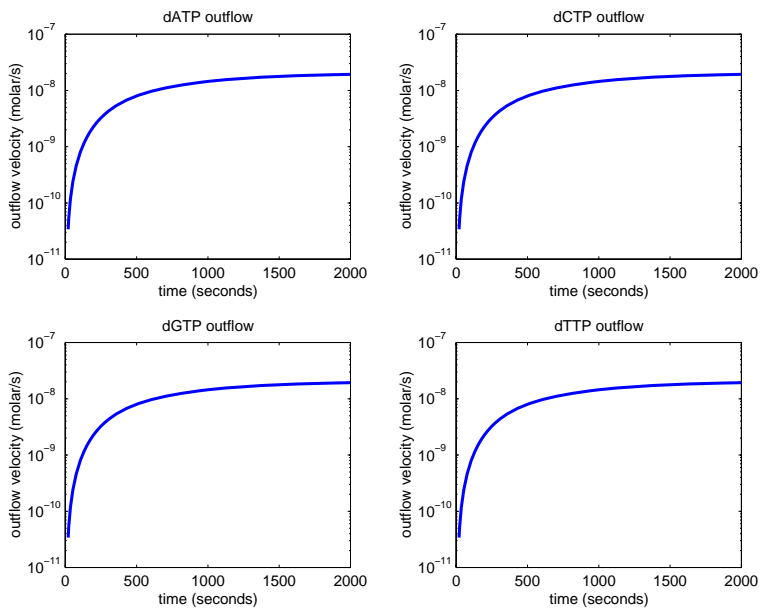


Figure 12: Outflow of dNTPs to replication. This is the flow described by equation 31. Simulation with parameters shown in table 5.

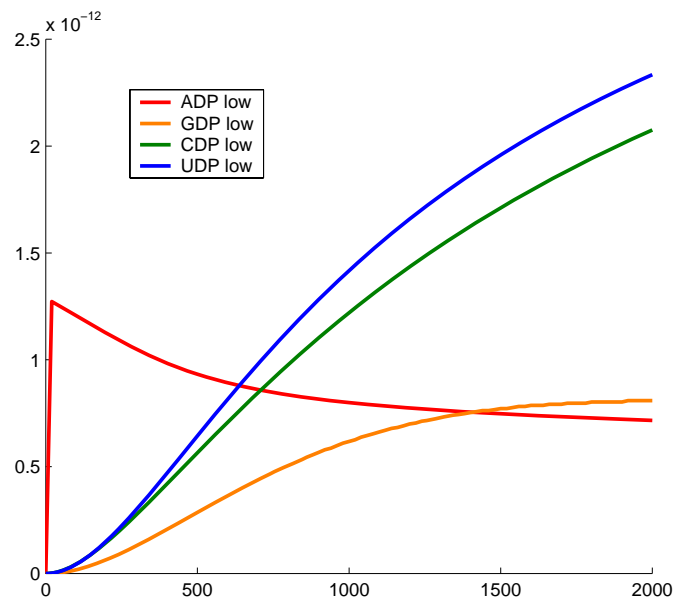


Figure 13: Outflow of dNTPs to replication with different NDPs in low inflow concentration. In each case, NDP inflow was changed from a standard level of $50 \mu\text{M}$ to $0.001 \mu\text{M}$, that is virtually depleting it. Y-axis: concentration (M), X-axis: time (s).

Parameter	Value
$K_{m,CDP}$	180 μM
$K_{m,UDP}$	220 μM
$K_{m,GDP}$	25 μM
$K_{m,ADP}$	30 μM
$k_{cat,CDP}$	0.3 s^{-1}
$k_{cat,UDP}$	0.25 s^{-1}
$k_{cat,GDP}$	0.17 s^{-1}
$k_{cat,ADP}$	0.17 s^{-1}
$K_{d,dATP,ACT}$	6 μM
$K_{d,dATP,SPEC}$	0.43 μM
$K_{d,ATP,ACT}$	80 μM
$K_{d,ATP,SPEC}$	80 μM
$K_{d,dTTP,SPEC}$	1.9 μM
$K_{d,dGTP,SPEC}$	0.77 μM
$K_{m,pol,dATP}$	4 μM
$K_{m,pol,dCTP}$	5 μM
$K_{m,pol,dGTP}$	4 μM
$K_{m,pol,dTTP}$	2 μM
k_{repl}	1000 s^{-1}
D	2
$[RNR]_{tot}$	1 μM
k_T	10 s^{-1}
K_C	1 μM
K_T	1 μM
ATP	3 mM

Table 5: Parameter values used in the model.

APPENDIX 1: MATLAB Code

```
% UNITS
% Concentration: micromolar
% Time: seconds

clear all
close all

% SIMULATION PARAMETERS

RUNS_outer = 100;
RUNS_inner = 400;
DT = 0.05;
time_steps = RUNS_outer*RUNS_inner;

% Initiate vectors
dATPs = zeros(1, RUNS_outer+1);
ATPs = zeros(1, RUNS_outer+1);
dCTPs = zeros(1, RUNS_outer+1);
dGTPs = zeros(1, RUNS_outer+1);
dTTPs = zeros(1, RUNS_outer+1);

act_dATPs = zeros(1, RUNS_outer+1);
act_ATPs = zeros(1, RUNS_outer+1);
spec_dATPs = zeros(1, RUNS_outer+1);
spec_ATPs = zeros(1, RUNS_outer+1);
spec_dGTPs = zeros(1, RUNS_outer+1);
spec_dTTPs = zeros(1, RUNS_outer+1);
spec_frees = zeros(1, RUNS_outer+1);
act_frees = zeros(1, RUNS_outer+1);

ADPs = zeros(1, RUNS_outer+1);
GDPs = zeros(1, RUNS_outer+1);
CDPs = zeros(1, RUNS_outer+1);
UDPs = zeros(1, RUNS_outer+1);

RNR_GDPs = zeros(1, RUNS_outer+1);
RNR_ADPs = zeros(1, RUNS_outer+1);
RNR_CDP_UDPs = zeros(1, RUNS_outer+1);
RNR_inhibs = zeros(1, RUNS_outer+1);

dATP_decrs = zeros(1, RUNS_outer+1);
dCTP_decrs = zeros(1, RUNS_outer+1);
dGTP_decrs = zeros(1, RUNS_outer+1);
dTTP_decrs = zeros(1, RUNS_outer+1);
dATP_incrs = zeros(1, RUNS_outer+1);
dCTP_incrs = zeros(1, RUNS_outer+1);
dGTP_incrs = zeros(1, RUNS_outer+1);
dTTP_incrs = zeros(1, RUNS_outer+1);

t = zeros(1, RUNS_outer+1);

% ENZYME REACTION CONSTANTS

Km_CDP = 180;
Km_UDP = 220;
Km_GDP = 25;
```

```

Km_ADP = 30;

kcat_CDP = 0.3;
kcat_UDP = 0.25;
kcat_GDP = 0.17;
kcat_ADP = 0.17;

mu = 1e-4;

% EFFECTOR DISSOCIATION CONSTANTS

Kd_dATP_act      = 6;           % Reference: Urmö-Sjöberg 1990, p. 140
Kd_dATP_spec     = 0.43;
Kd_ATP_act       = 80;
Kd_ATP_spec      = 80;
Kd_dTTP          = 1.9;
Kd_dGTP          = 0.77;

% DNA POLYMERASE CONSTANTS

pol_Km_dATP = 4;
pol_Km_dCTP = 5;
pol_Km_dGTP = 4;
pol_Km_dTTP = 2;

O = zeros(1, time_steps/4);
I = 0.25*ones(1, time_steps/4);
f_dATP = [I I I I];
f_dCTP = [I I I I];
f_dGTP = [I I I I];
f_dTTP = [I I I I];

k_repl = 1000;

D = 10^-1; % Replication site concentration

% INITIAL CONCENTRATIONS

RNR_tot = 1;

% Effector-site concentrations
act_ATP   = 0;
act_dATP  = 0;
act_free  = RNR_tot - act_ATP - act_dATP;
spec_ATP  = 0;
spec_dATP = 0;
spec_dTTP = 0;
spec_dGTP = 0;
spec_free = RNR_tot - spec_ATP - spec_dATP - spec_dTTP - spec_dGTP;

% RNR concentrations, calculated from
% the effector-site concentrations
RNR_GDP   = act_ATP * spec_dTTP / RNR_tot;
RNR_ADP   = act_ATP * spec_dGTP / RNR_tot;
RNR_CDP_UDP = act_ATP * (spec_ATP + spec_dATP) / RNR_tot;
RNR_inhib = RNR_tot - RNR_GDP - RNR_ADP - RNR_CDP_UDP;

dATP = 0; % dNTP concentrations
dTTP = 0;
dGTP = 0;

```

```

dCTP = 0;

ATP = 3000; % ND(T)P concentrations
CDP = 50;
UDP = 50;
GDP = 50;
ADP = 0.001;

dATP_tot = dATP + act_dATP + spec_dATP;
ATP_tot = ATP + act_ATP + spec_ATP;
dGTP_tot = dGTP + spec_dGTP;
dTTP_tot = dTTP + spec_dTTP;

% Adjust effector and effector-site equilibrium concentrations

current_conc = [dATP, ATP, dGTP, dTTP, act_dATP, act_ATP, spec_dATP, spec_ATP, spec_dGTP, spec_dTTP, act_free, spec_free];
K = [Kd_dATP_act, Kd_dATP_spec, Kd_ATP_act, Kd_ATP_spec, Kd_dTTP, Kd_dGTP];
tot_conc = [dATP_tot, ATP_tot, dGTP_tot, dTTP_tot, RNR_tot];

new_conc = eq_conc_aerobic(current_conc, K, tot_conc);

dATP = new_conc(1); ATP = new_conc(2); dGTP = new_conc(3); dTTP = new_conc(4); act_dATP = new_conc(5);
act_ATP = new_conc(6); spec_dATP = new_conc(7); spec_ATP = new_conc(8); spec_dGTP = new_conc(9);
spec_dTTP = new_conc(10); act_free = new_conc(11); spec_free = new_conc(12);

% Store conc. values
dATPs(1) = dATP; ATPs(1) = ATP; dCTPs(1) = dCTP; dGTPs(1) = dGTP; dTTPs(1) = dTTP; act_ATPs(1) = act_ATP;
spec_dATPs(1) = spec_dATP; spec_ATPs(1) = spec_ATP; spec_dGTPs(1) = spec_dGTP; spec_dTTPs(1) = spec_dTTP;
spec_frees(1) = spec_free; act_frees(1) = act_free;
ADPs(1) = ADP; GDPs(1) = GDP; CDPs(1) = CDP; UDPs(1) = UDP;
RNR_GDPs(1) = RNR_GDP; RNR_ADPs(1) = RNR_ADP; RNR_CDP_UDPs(1) = RNR_CDP_UDP; RNR_inhbs(1) = RNR_inhib;

t(1) = 0;

% SIMULATION

for j = 2:RUNS_outer+1
    j
    for i = 1:RUNS_inner

        ind = (j-2)*RUNS_inner + i;

        % Increase in dNTP concentrations from Michaelis-Menten reactions
        dATP_incr = ( RNR_ADP * ADP * kcat_ADP / (ADP + Km_ADP) ) * DT;
        dGTP_incr = ( RNR_GDP * GDP * kcat_GDP / (GDP + Km_GDP) ) * DT;
        dCTP_incr = ( RNR_CDP_UDP * CDP * kcat_CDP / (CDP + Km_CDP * (1 + UDP/Km_UDP)) ) * DT;
        dTTP_incr = ( RNR_CDP_UDP * UDP * kcat_UDP / (UDP + Km_UDP * (1 + CDP/Km_CDP)) ) * DT;

        % Decrease in dNTP concentrations from replication
        v = 1/( 1/k_repl*(f_dATP(ind)*(1 + pol_Km_dATP/dATP) + f_dGTP(ind)*(1 + pol_Km_dGTP/dGTP) + f_dCTP(ind)*(1 + pol.
        dATP_decr = f_dATP(ind)*D*v * DT;
        dGTP_decr = f_dGTP(ind)*D*v * DT;
        dCTP_decr = f_dCTP(ind)*D*v * DT;
        dTTP_decr = f_dTTP(ind)*D*v * DT;

        % Adjust concentrations

        dATP = dATP + dATP_incr - dATP_decr - mu*dATP*DT;
        dGTP = dGTP + dGTP_incr - dGTP_decr - mu*dGTP*DT;

```

```

dCTP = dCTP + dCTP_incr - dCTP_decr - mu*dCTP*DT;
dTTP = dTTP + dTTP_incr - dTTP_decr - mu*dTTP*DT;

% Flow from dCTP to dTTP
kT = 10;
KC = 1;
KT = 1;
EO = 0;
dTTP_change = EO*kT*dCTP/KC/(1 + dCTP/KC + dTTP/KT)*DT;
dCTP = dCTP - dTTP_change;
dTTP = dTTP + dTTP_change;

dATP_tot = dATP + act_dATP + spec_dATP;
ATP_tot = ATP + act_ATP + spec_ATP;
dGTP_tot = dGTP + spec_dGTP;
dTTP_tot = dTTP + spec_dTTP;

% Adjust effector and effector-site equilibrium concentrations

current_conc = [dATP, ATP, dGTP, dTTP, act_dATP, act_ATP, spec_dATP, spec_ATP, spec_dGTP, spec_dTTP, act_free, spec_free];
K = [Kd_dATP_act, Kd_dATP_spec, Kd_ATP_act, Kd_ATP_spec, Kd_dTTP, Kd_dGTP];
tot_conc = [dATP_tot, ATP_tot, dGTP_tot, dTTP_tot, RNR_tot];

new_conc = eq_conc_aerobic(current_conc, K, tot_conc);

dATP_change = new_conc(1) - dATP;
dGTP_change = new_conc(3) - dGTP;
dTTP_change = new_conc(4) - dTTP;

dATP = new_conc(1); ATP = new_conc(2); dGTP = new_conc(3); dTTP = new_conc(4); act_dATP = new_conc(5);
act_ATP = new_conc(6); spec_dATP = new_conc(7); spec_ATP = new_conc(8); spec_dGTP = new_conc(9);
spec_dTTP = new_conc(10); act_free = new_conc(11); spec_free = new_conc(12);

% RNR concentrations, calculated from
% the effector-site concentrations
RNR_GDP = act_ATP * spec_dTTP / RNR_tot;
RNR_ADP = act_ATP * spec_dGTP / RNR_tot;
RNR_CDP_UDP = act_ATP * (spec_ATP + spec_dATP) / RNR_tot;
RNR_inhib = RNR_tot - RNR_GDP - RNR_ADP - RNR_CDP_UDP;

end

% Store conc. values
dATPs(j) = dATP;
ATPs(j) = ATP;
dCTPs(j) = dCTP;
dGTPs(j) = dGTP;
dTTPs(j) = dTTP;

act_dATPs(j) = act_dATP;
act_ATPs(j) = act_ATP;
spec_dATPs(j) = spec_dATP;
spec_ATPs(j) = spec_ATP;
spec_dGTPs(j) = spec_dGTP;
spec_dTTPs(j) = spec_dTTP;
spec_frees(j) = spec_free;
act_frees(j) = act_free;

ADPs(j) = ADP;
GDPs(j) = GDP;
CDPs(j) = CDP;

```

```

UDPs(j) = UDP;

RNR_GDPs(j) = RNR_GDP;
RNR_ADPs(j) = RNR_ADP;
RNR_CDP_UDPs(j) = RNR_CDP_UDP;
RNR_inhibs(j) = RNR_inhib;

dATP_decrs(j) = dATP_decr;
dCTP_decrs(j) = dCTP_decr;
dGTP_decrs(j) = dGTP_decr;
dTTP_decrs(j) = dTTP_decr;
dATP_incrs(j) = dATP_incr;
dCTP_incrs(j) = dCTP_incr;
dGTP_incrs(j) = dGTP_incr;
dTTP_incrs(j) = dTTP_incr;

dATP_tots(j) = dATP_tot;
ATP_tots(j) = ATP_tot;
dGTP_tots(j) = dGTP_tot;
dTTP_tots(j) = dTTP_tot;

dATP_changes(j) = dATP_change;
dGTP_changes(j) = dGTP_change;
dTTP_changes(j) = dTTP_change;

t(j) = DT*(j-1)*RUNS_inner;

end

figure
semilogy(t,dATPs/10^6, t,dCTPs/10^6,t,dGTPs/10^6,t,dTTPs/10^6)
legend('dATP','dCTP','dGTP','dTTP')
xlabel('time (seconds)')
ylabel('concentration (molar)')
title('dNTP pools')

figure
subplot(2,2,1)
semilogy(t,dATPs/10^6,'LineWidth',2)
xlabel('time (seconds)')
ylabel('concentration (molar)')
title('dATP')
subplot(2,2,2)
semilogy(t,dCTPs/10^6,'LineWidth',2)
xlabel('time (seconds)')
ylabel('concentration (molar)')
title('dCTP')
subplot(2,2,3)
semilogy(t,dGTPs/10^6,'LineWidth',2)
xlabel('time (seconds)')
ylabel('concentration (molar)')
title('dGTP')
subplot(2,2,4)
semilogy(t,dTTPs/10^6,'LineWidth',2)
xlabel('time (seconds)')
ylabel('concentration (molar)')
title('dTTP')

figure
subplot(2,2,1)
semilogy(t,ADPs/10^6,'LineWidth',2)

```

```

xlabel('time (seconds)')
ylabel('concentration (molar)')
title('ADP')
subplot(2,2,2)
semilogy(t,CDPs/10^6,'LineWidth',2)
xlabel('time (seconds)')
ylabel('concentration (molar)')
title('CDP')
subplot(2,2,3)
semilogy(t,GDPs/10^6,'LineWidth',2)
xlabel('time (seconds)')
ylabel('concentration (molar)')
title('GDP')
subplot(2,2,4)
semilogy(t,UDPs/10^6,'LineWidth',2)
xlabel('time (seconds)')
ylabel('concentration (molar)')
title('UDP')

figure
semilogy(t,ATPs/10^6)
legend('ATP')
xlabel('time (seconds)')
ylabel('concentration (molar)')
title('ATP concentration')

figure
semilogy(t,spec_frees/10^6,'-',t,spec_ATPs/10^6,':',t,spec_dATPs/10^6,'-.',t,spec_dGTPs/10^6,'--',t,spec_dTTPs/10^6)
legend('free','ATP bound','dATP bound','dGTP bound','dTTP bound')
xlabel('time (seconds)')
ylabel('concentration (molar)')
title('Specificity site')

figure
semilogy(t,act_frees/10^6,'-',t,act_ATPs/10^6,'--',t,act_dATPs/10^6,'-.')
legend('free','ATP bound','dATP bound')
xlabel('time (seconds)')
ylabel('concentration (molar)')
title('Activity site')

figure
subplot(2,2,1)
semilogy(t,RNR_GDPs/10^6,'LineWidth',2)
xlabel('time (seconds)')
ylabel('concentration (molar)')
title('GDP-reducing RNR')
subplot(2,2,2)
semilogy(t,RNR_ADPs/10^6,'LineWidth',2)
xlabel('time (seconds)')
ylabel('concentration (molar)')
title('ADP-reducing RNR')
subplot(2,2,3)
semilogy(t,RNR_CDP_UDPs/10^6,'LineWidth',2)
xlabel('time (seconds)')
ylabel('concentration (molar)')
title('CDP- and UDP-reducing RNR')
subplot(2,2,4)
semilogy(t,RNR_inhibs/10^6,'LineWidth',2)
xlabel('time (seconds)')
ylabel('concentration (molar)')
title('Inhibited')

```

```

figure
subplot(2,2,1)
semilogy(t,dATP_decrs/DT/10^6,'LineWidth',2)
xlabel('time (seconds)')
ylabel('outflow velocity (molar/s)')
title('dATP outflow')
subplot(2,2,2)
semilogy(t,dCTP_decrs/DT/10^6,'LineWidth',2)
xlabel('time (seconds)')
ylabel('outflow velocity (molar/s)')
title('dCTP outflow')
subplot(2,2,3)
semilogy(t,dGTP_decrs/DT/10^6,'LineWidth',2)
xlabel('time (seconds)')
ylabel('outflow velocity (molar/s)')
title('dGTP outflow')
subplot(2,2,4)
semilogy(t,dTTP_decrs/DT/10^6,'LineWidth',2)
xlabel('time (seconds)')
ylabel('outflow velocity (molar/s)')
title('dTTP outflow')

```

```

figure
subplot(2,2,1)
semilogy(t,dATP_incrs/DT/10^6,'LineWidth',2)
xlabel('time (seconds)')
ylabel('inflow velocity (molar/s)')
title('dATP outflow')
subplot(2,2,2)
semilogy(t,dCTP_incrs/DT/10^6,'LineWidth',2)
xlabel('time (seconds)')
ylabel('inflow velocity (molar/s)')
title('dCTP outflow')
subplot(2,2,3)
semilogy(t,dGTP_incrs/DT/10^6,'LineWidth',2)
xlabel('time (seconds)')
ylabel('inflow velocity (molar/s)')
title('dGTP outflow')
subplot(2,2,4)
semilogy(t,dTTP_incrs/DT/10^6,'LineWidth',2)
xlabel('time (seconds)')
ylabel('inflow velocity (molar/s)')
title('dTTP outflow')

```

```

figure
semilogy(t,dATP_tots/10^6,'-',t,ATP_tots/10^6,':',t,dGTP_tots/10^6,'-',t,dTTP_tots/10^6,'--')
legend('TOT dATP','TOT ATP','TOT dGTP','TOT dTTP')
xlabel('time (seconds)')
ylabel('concentration (molar)')
title('TOTAL CONC')

```

```

figure
semilogy(t,dATP_tots/10^6,'-',t,ATP_tots/10^6,':',t,dGTP_tots/10^6,'-',t,dTTP_tots/10^6,'--')
legend('TOT dATP','TOT ATP','TOT dGTP','TOT dTTP')
xlabel('time (seconds)')
ylabel('concentration (molar)')
title('TOTAL CONC')

```

```

figure
semilogy(t,abs(dATP_changes)/DT/10^6,'-',t,abs(dGTP_changes)/DT/10^6,'-',t,abs(dTTP_changes)/DT/10^6,'--')
legend('dATP','dGTP','dTTP')
xlabel('time (seconds)')

```

```
ylabel('concentration (molar)')  
title('CONC CHANGES')
```

APPENDIX 2: Computational Methods

Calculation of RNR Concentrations

Given probabilities for effector binding at the allosteric sites, we can calculate RNR concentrations. Each probability can be expressed on the following form, *i.e.* the fraction of enzyme with a specific effector bound, to the total enzyme concentration:

$$P(\text{ATP at ACT site}) = \frac{[ACT_{ATP}]}{[RNR]_{tot}} \quad (1)$$

The expression is the same for the other effectors. Substituting these probabilities into the expressions for the probabilities of NDP reduction (equations (21) to (24)), yields for example from equation (21):

$$P(\text{ADP reduction}) = \frac{[ACT_{ATP}][SPEC_{dGTP}]}{[RNR]_{tot}^2} \quad (2)$$

Now we can multiply with $[RNR]_{tot}$ to get the concentration of ADP-reducing RNR. Doing this for all probabilities yields equations (26) to (29).

External Control

From the scheme given in figure 3 and the definitions of constants given there, we can write the flow to dTTP over the enzyme as

$$j = ECk_T \quad (3)$$

The dissociation constants are:

$$K_C = \frac{E \cdot C}{EC} \quad (4)$$

$$K_T = \frac{E \cdot T}{ET} \quad (5)$$

This means that the total enzyme concentration can be written:

$$E_0 = E + EC + ET = E(1 + C/K_C + T/K_T) \quad (6)$$

which yields an expression for the concentration of free enzyme. Solving for EC and substituting into the expression for the flow yields the following expression:

$$j = ECk_T = \frac{E_0 k_T C / K_C}{1 + C/K_C + T/K_T} \quad (7)$$

Replication Model

The flow j_{repl} of dNTP into DNA is the product of the number of replication forks D replicating the chromosome, the fraction f_i of the dNTP i in all DNA in the cell and the average replication speed v .

$$j_{repl, dnTP} = f_{dnTP} D v, n = A, C, G, T \quad (8)$$

The replication speed v is the reverse of the average time τ it takes to incorporate any of the four bases into DNA:

$$\frac{1}{v} = \tau = \sum_{n=A,C,G,T} f_{dnTP} \tau_{dnTP} \quad (9)$$

Assuming Michaelis-Menten kinetics for the replication, the average time to incorporate each base is given by

$$\tau_{dnTP} = \frac{1}{c_{dnTP}} = \frac{1}{k_{repl, dnTP}} \left(1 + \frac{K_{pol, dnTP}}{[dnTP]} \right) \quad (10)$$

where $k_{repl,dnTP}$ and $K_{pol,dnTP}$ are Michaelis-Menten constants for each base. Assuming the maximal rate is the same for all bases (k_{repl}) and inserting (10) and (9) into (8) the outflow from each dNTP pool into replication is

$$j_{repl,dnTP} = \frac{f_{dnTP}D}{\frac{1}{k_{repl}} \sum_{i=A,C,G,U} (f_{diTP} (1 + \frac{K_{m,pol,diTP}}{[diTP]}))}, \quad (11)$$

$n = A, C, G, U$